Development 134, 211-222 (2007) doi:10.1242/dev.02700

The maturation of mucus-secreting gastric epithelial progenitors into digestive-enzyme secreting zymogenic cells requires *Mist1*

Victoria G. Ramsey[1,*], Jason M. Doherty[1,*], Christopher C. Chen[1], Thaddeus S. Stappenbeck[1,2], Stephen F. Konieczny[3] and Jason C. Mills[1,2,†]

Continuous regeneration of digestive enzyme (zymogen)-secreting chief cells is a normal aspect of stomach function that is disrupted in precancerous lesions (e.g. metaplasias, chronic atrophy). The cellular and genetic pathways that underlie zymogenic cell (ZC) differentiation are poorly understood. Here, we describe a gene expression analysis of laser capture microdissection purified gastric cell populations that identified the bHLH transcription factor *Mist1* as a potential ZC regulatory factor. Our molecular and ultrastructural analysis of proliferation, migration and differentiation of the gastric unit in *Mist1*$^{-/-}$ and control mice supports a model whereby wild-type ZC progenitors arise as neck cells in the proliferative (isthmal) zone of the gastric unit and become transitional cells (TCs) with molecular and ultrastructural characteristics of both enzyme-secreting ZCs and mucus-secreting neck cells as they migrate to the neck-base zone interface. Thereafter, they rapidly differentiate into mature ZCs as they enter the base. By contrast, *Mist1*$^{-/-}$ neck cells differentiate normally, but ZCs in the mature, basal portion of the gastric unit uniformly exhibit multiple apical cytoplasmic structural abnormalities. This defect in terminal ZC differentiation is also associated with markedly increased abundance of TCs, especially in late-stage TCs that predominantly have features of immature ZCs. Thus, we present an in vivo system for analysis of ZC differentiation, present molecular evidence that ZCs differentiate from neck cell progenitors and identify *Mist1* as the first gene with a role in this clinically important process.

KEY WORDS: Bhlhb8, Mucous neck cell, Laser-capture microdissection, Microarray, Mouse

INTRODUCTION

Key functions of the mammalian stomach epithelium are to secrete acid, digestive enzymes and mucus. Cells that perform those tasks are located within repeating glandular invaginations, known as gastric units (Fig. 1A). All gastric epithelial cells turn over throughout life and are constantly replenished by differentiation from an adult stem cell residing in each unit (Fig. 1B). Detailed morphological studies of differentiation (Karam, 1993; Karam and Leblond, 1993d; Karam and Leblond, 1993c; Karam and Leblond, 1993b; Karam et al., 2003) have revealed that the gastric unit in the stomach corpus (body) can be organized by anatomy and cell function into: the pit zone, which opens into the gastric lumen and is lined by mucus-secreting pit cells; the isthmus, which houses the stem cell; the neck zone, which contains mucus-secreting neck cells located among acid-secreting parietal cells; and the base zone, which contains digestive enzyme-secreting zymogenic cells (ZCs) (Fig. 1). The developmental pathways characteristic of the adult gastric epithelium are established postnatally: the ZC lineage, the last to appear, emerges at ~3 weeks of age in mice (Li et al., 1996).

Gastric epithelial differentiation is strongly correlated with migration (Fig. 1B). Specific cell lineages must execute the proper spatial (i.e. toward the lumen or base) and temporal program. The mucus-secreting cells of the neck, for example, mature as they descend over ~14 days toward the base of the gastric unit. By contrast, pit cells mature along a more short-lived (~3 days in mice) gradient climbing toward the gastric lumen. Acid-secreting parietal cells arise in the isthmus, and most thereafter migrate into the neck zone, where they live ~54 days in mice (Karam et al., 1997).

The most poorly understood differentiation pathway in the gastric unit is that of the ZC, which is found only in the base zone but, like all gastric epithelial cells, continuously turns over (half-life, 194 days) and must be replenished by the stem cell in the isthmus. Morphological studies (Suzuki et al., 1983; Karam and Leblond, 1993c; Ge et al., 1998) suggest that ZCs arise from mucous neck cells that migrate into the base zone. However, this neck-to-ZC transition hypothesis has been recently called into question (Hanby et al., 1999). The reason for the skepticism is that if neck cells transition into ZCs, they must first form an elaborate mucus-secretory apparatus that they then must dismantle, shed or convert, as they subsequently construct the equally elaborate serous secretory apparatus characteristic of the mature ZC (Fig. 1C). The cell and molecular processes that could convert a postmitotic, fully functional mucus-secreting cell into a zymogen-secreting cell with a different function have not previously been described.

In this report, we analyze ZC differentiation at the molecular level to identify potential factors that might regulate the neck-to-ZC transition. We developed an RNA-preserving approach for laser-capture microdissection (LCM)-based purification of individual gastric epithelial cell lineages, generated gene expression profiles from each lineage, and performed a bioinformatic screen that targeted one high probability candidate regulator of ZC differentiation. The candidate, *Mist1* (*Bhlhb8* – Mouse Genome Informatics), encodes a class B basic helix-loop-helix transcription factor previously shown to be expressed in only a handful of specialized secretory cell lineages, such as acinar cells of the salivary

[1]Department of Pathology and Immunology and [2]Department of Molecular Biology and Pharmacology, Washington University School of Medicine, St Louis, MO 63110, USA. [3]Department of Biological Sciences and the Purdue Cancer Center, Purdue University, West Lafayette, Indiana 47907-2064, USA.

*These authors contributed equally to this work
†Author for correspondence (e-mail: jmills@pathology.wustl.edu)

Accepted 18 October 2006

gland and pancreas (Pin et al., 2000; Johnson et al., 2004). Molecular and genetic studies have shown that formation of Mist1 homodimers is crucial for Ca^{2+}-regulated exocytosis and intercellular communication in acinar tissues (Pin et al., 2001; Rukstalis et al., 2003; Zhu et al., 2004; Luo et al., 2005).

Therefore, we hypothesized a regulatory role for *Mist1* in ZC differentiation and, thus, performed quantitative and qualitative molecular and ultrastructural analyses of gastric unit development in *Mist1*$^{-/-}$ mice. We find that normal, mature ZCs do not form in the bases of *Mist1*$^{-/-}$ gastric units. Rather, basal *Mist1*$^{-/-}$ ZCs have markedly underdeveloped apical cytoplasms with multiple ultrastructural defects. In the absence of normal ZCs, there is accumulation – at the transition between neck and base zones – of cells with features of both neck and zymogenic cells. Although increased in abundance, these transitional cells are otherwise normal. Thus, our results provide molecular and cellular evidence that ZCs do in fact arise from neck cells. Furthermore, we identify *Mist1* as the first gene necessary for this maturation process and present evidence that Mist1 specifically regulates genes involved in extension of the apical cytoplasm, which we identify as a key feature of normal ZC differentiation from neck cells.

MATERIALS AND METHODS

Mice

All experiments involving animals were performed according to protocols approved by the Washington University School of Medicine Animal Studies Committee. Mice were maintained in a specified-pathogen-free barrier facility under a 12 hour light cycle. Germline *Mist1*$^{-/-}$ mice were generated as described previously (Pin et al., 2001). Tissue for the LCM/GeneChip studies was dissected from stomachs of wild-type FVB/N mice (The Jackson Laboratory, Bar Harbor, ME, USA).

RNA-preserving triple channel immunolabeling for LCM

Stomachs for LCM were excised immediately following sacrifice, quickly flushed with RT PBS, inflated by duodenal injection of O.C.T. (Sakura Finetek, Torrance, CA), and frozen in Cytocool II (Richard-Allen Scientific, Kalamazoo, MI). Serial 7 μm-thick cryosections were cut onto Superfrost slides (Fisher Scientific), fixed in 70% ETOH, rehydrated in nuclease-free water (nuclease-free solutions from Ambion, Austin, TX) and then incubated in immunolabeling buffer. Several buffers and incubation times for multichannel, fluorescent immunolabeling cell lineages were tested. Although labeling was optimal in nuclease-free PBS, these conditions led to activation of endogenous gastric RNases and complete degradation of RNA within 5 minutes (RNA integrity assessed by Agilent 2100 Bioanalyzer, Palo Alto, CA). RNA preservation was enhanced in buffers with lower pH (e.g. Sodium Acetate, pH 4.3, prepared in nuclease-free water) and/or lower ionic strength (e.g. 10 mmol/l nuclease-free Tris-HCl, multiple pHs from 5-7). However, the optimal balance of preservation and labeling occurred by diluting all immunolabeling reagents in unbuffered, nuclease-free water with total incubation time no longer than 30 minutes. For the current studies, reagents for triple-labeling were: (1) to identify parietal cells, 20 μg/ml AlexaFluor532-labeled (Molecular Probes, Eugene, OR) *Dolichos biflorus* agglutinin (DBA) lectin (E-Y Laboratories, San Mateo, CA); (2) to label neck cells (Falk et al., 1994), 20 μg/ml Alexafluor488-labeled *Griffonia simplicifolia II* (Molecular Probes); (3) to identify pit cells and ZCs, 10 μg/ml mouse anti-E-cadherin (BD Biosciences), prelabeled using the Alexafluor647 IgG2a mouse Zenon primary antibody labeling kit (Molecular Probes). After labeling, slides were alcohol or xylene dehydrated and stored in desiccation chambers (no more than 3 hours) until LCM was performed.

LCM and GeneChips

Individual parietal cells (visualized by DBA-positivity and autofluorescence) from well-oriented gastric units were dissected (PixCell II LCM apparatus, 7.5 μm spot diameter; CapSure HS LCM caps, Arcturus, Mountain View, CA) one at a time from the pit zone and collected for GeneChips. Pit cells (E-cadherin-positive, DBA-negative) were then collected from the same gastric units. Only the pit cells in a two- to three-cell-thick region at the apex of the gastric unit – but not yet upon the gastric surface – were taken. ZCs (E-cadherin-positive, GSII/DBA-negative cells in the base zones) were collected from corpus gastric units after potentially contaminating basal parietal cells had first been dissected and discarded. Between 3000 and 5000 individual cells from each cell lineage were isolated from four to five individual mice. RNA was purified by PicoPure kit (Arcturus). RNA integrity was verified, and RNAs for each lineage were pooled from multiple mice, and 10 ng total RNA was then amplified, labeled and fragmented (by the Arcturus RiboAmp HS kit followed by the RNA Amplification and Labeling Kit from Enzo Life Sciences). The resulting biotinylated cRNA probes were hybridized to Affymetrix (Santa Clara, CA) MOE430v2 GeneChips.

Bioinformatic analysis

Chip quality control and GeneChip to GeneChip comparisons to generate expression profiles were performed using dChip (Li and Wong, 2001; Zhong et al., 2003). Cell lineage-specific profiles were generated by extracting those genes whose expression was increased in the given cell lineage relative to the other two cell lineages (parameters: lower bound of 90% confidence of fold-change ⩾1.3, expression intensity difference ⩾50). The length (in number of probesets) of each expression profile was as follows: LCM ZC (1066), LCM parietal cell (665), LCM Pit (469), Previous ZC (1121), Previous parietal cell (285), Previous Pit (701). To compare these expression profiles across different versions of Affymetrix GeneChips and different microarray platforms, each expression profile (i.e. the list of genes with expression that was increased in each cell population) was re-expressed as a function of the Gene Ontology (GO) terms represented in each list, and then compared to all others on the basis of overall GO term distributions using the GOurmet software (Doherty et al., 2006).

Multi-organ GeneChip comparisons

To identify which of the 41 candidate regulators of ZC differentiation were preferentially expressed in salivary gland, we performed head-to-head comparisons (parameters: fold-change lower bound ⩾1.2, intensity difference ⩾100) between the salivary gland and all other organs (excluding stomach) from a panel of 15 mouse organs (RC Lindsley and KM Murphy, contributors; GEO Series GSE1986; http://www.ncbi.nlm.nih.gov/geo/query/acc.cgi?acc=GSE1986). Only two of the 41 genes were expressed preferentially in salivary gland: one probe set for *Mist1* and three independent probe sets all representing *Xbp1*.

Antibodies and immunostaining

Primary antibodies used for the non-LCM experiments in this study: rabbit (1:10,000) and goat (1:2000) anti-human gastric intrinsic factor (gifts of Dr David Alpers, Washington University), monoclonal mouse-anti-β-galactosidase (1:50), monoclonal mouse anti-Tff2 IgM (1:10, gift of Sir Nicholas Wright), sheep anti-PepsinogenC (Pgc 1:10,000, from Abcam), rabbit anti-Mist1 (1:200, described previously in Pin et al. (Pin et al., 2001), goat anti-Brdu (1:20,000, gift of Dr Jeff Gordon). Secondary antibodies for non-LCM immunofluorescence were: AlexaFluor (488, 594 or 647) conjugated donkey anti-goat, anti-rabbit, anti-sheep or anti-mouse (1:200-1:500, Molecular Probes).

Stomachs for immunofluorescent analysis were excised immediately, flushed with RT PBS via the duodenal stub and then inflated with freshly prepared methacarn fixative. The stub was clamped by hemostat, and the stomach suspended in fixative in a 150 ml Erlenmeyer flask for 15-30 minutes at RT, followed by multiple rinses in 70% ETOH, arrangement in 2% agar in a tissue cassette, and routine paraffin processing. Sections (5 μm) were cut, deparaffinized and rehydrated with graded xylenes, alcohols and water, then antigen-retrieved by boiling in 50 mmol/l Tris-HCl, pH 8.0 (9.0 for Mist1). Slides were blocked in 1% BSA, 0.3% Triton-X100, in PBS, then incubated overnight at 4°C in primary antibodies, rinsed in PBS, incubated 1 hour at RT in secondary antibodies and/or 1 μg/ml fluorescently labeled GSII lectin (Alexafluor488, 594 from Molecular Probes, Alexafluor647 made by directly conjugating E-Y Labs lectin to Molecular Probes Alexauor647), rinsed in PBS, incubated 5 minutes in 1 μg/ml bisbenzimide (Molecular Probes), and mounted in glycerol:PBS.

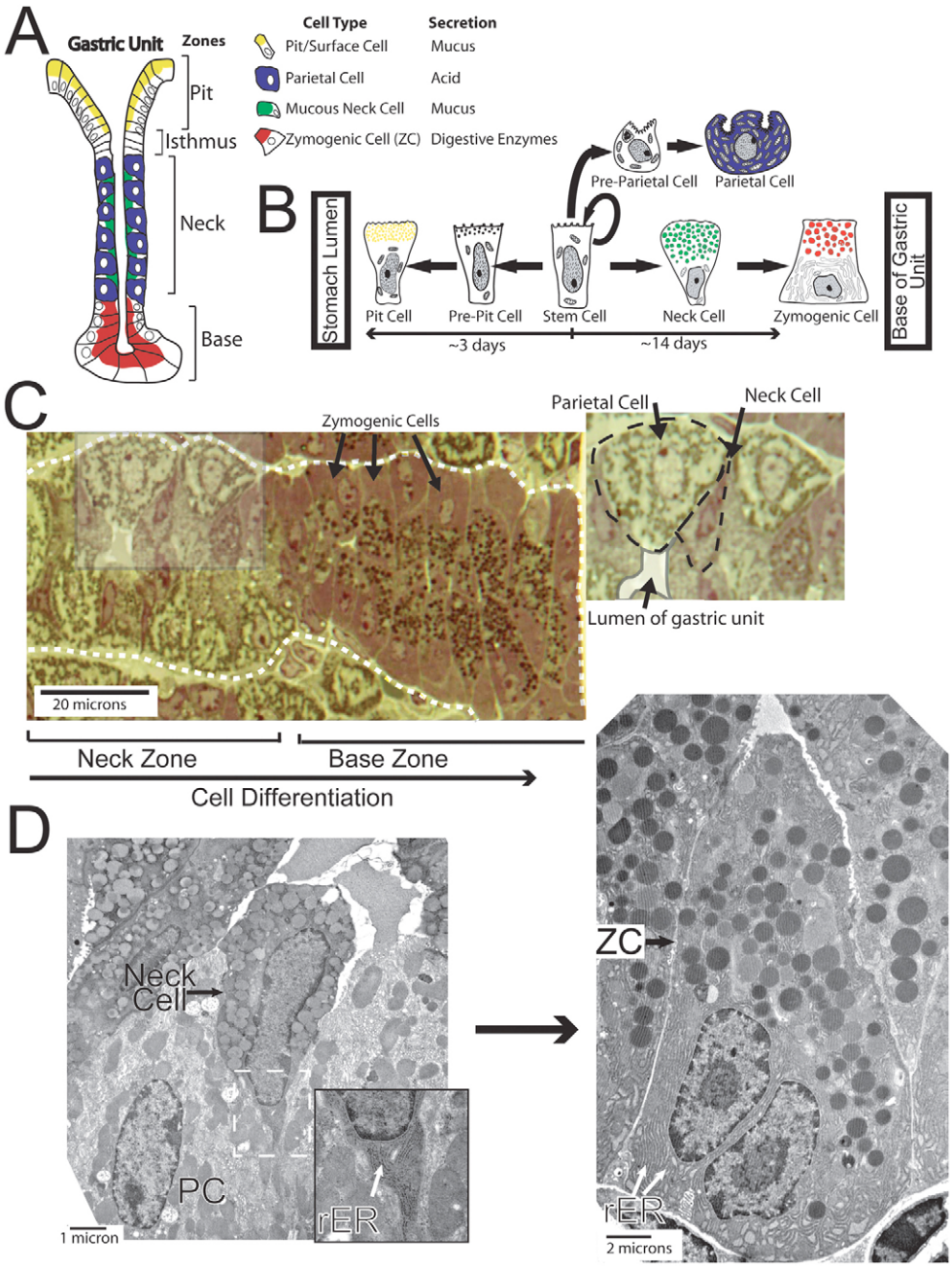

Fig. 1. Normal developmental pathways in the gastric unit of the adult stomach. (**A**) The epithelium of the corpus (body) consists of repeating, invaginating units that can be further subdivided into four zones: the pit, composed of mucus-secreting pit cells; the isthmus, where the multipotent stem cell resides; the neck where the mucous neck cells and the vast majority of the acid-secreting parietal cells reside; and the base, filled with digestive-enzyme-secreting zymogenic cells. (**B**) Key differentiation pathways in the gastric unit are depicted, with the gastric lumen to the left. The parietal cell arises within the isthmus. Pit and neck or zymogenic cells develop along well-defined, spatiotemporally organized developmental gradients. Neck cells are thought to enter the base and then become ZCs. (**C**) The neck and base of a single unit are depicted (unit delimited by white dashed line) in this Toluidine Blue-stained, 1 μm plastic-embedded section, oriented as in the cartoon in B. Inset: shaded rectangle in the neck zone of the photomicrograph at left with the gastric unit lumen outlined in gray. (**D**) TEM showing a typical neck cell (left) and a typical basal (i.e. mature) zymogenic cell (right). Inset: cytoplasmic projection of neck cell stretching between adjacent parietal cells (one labeled PC); note the nascent network of rER (arrow), which must become the extensive lamellar network in the mature zymogenic cell.

Immunofluorescence quantification

Stomachs from seven *Mist1*$^{-/-}$ and seven *Mist1*$^{+/-}$ littermates were fluorescently stained with bisbenzimide, and the following combinations of neck and ZC markers: GSII+anti-GIF, GSII+anti-Pgc, Tff2+anti-GIF. Photomicrographs (output as TIFF files from a Zeiss Axiovert 200 microscope with Axiocam MRM camera and with Apotome optical sectioning filter) from 10-13 well-oriented gastric units from each genotype and staining combination were randomly selected. All cells positive for neck and/or ZC markers were numbered as a function of increasing distance from the stem cell zone. The mean fluorescent intensity (MFI) was determined by manually outlining the cytoplasm of each cell and measuring mean 8 bit grayscale pixel intensity in the neck cell marker channel (e.g. GSII) and then

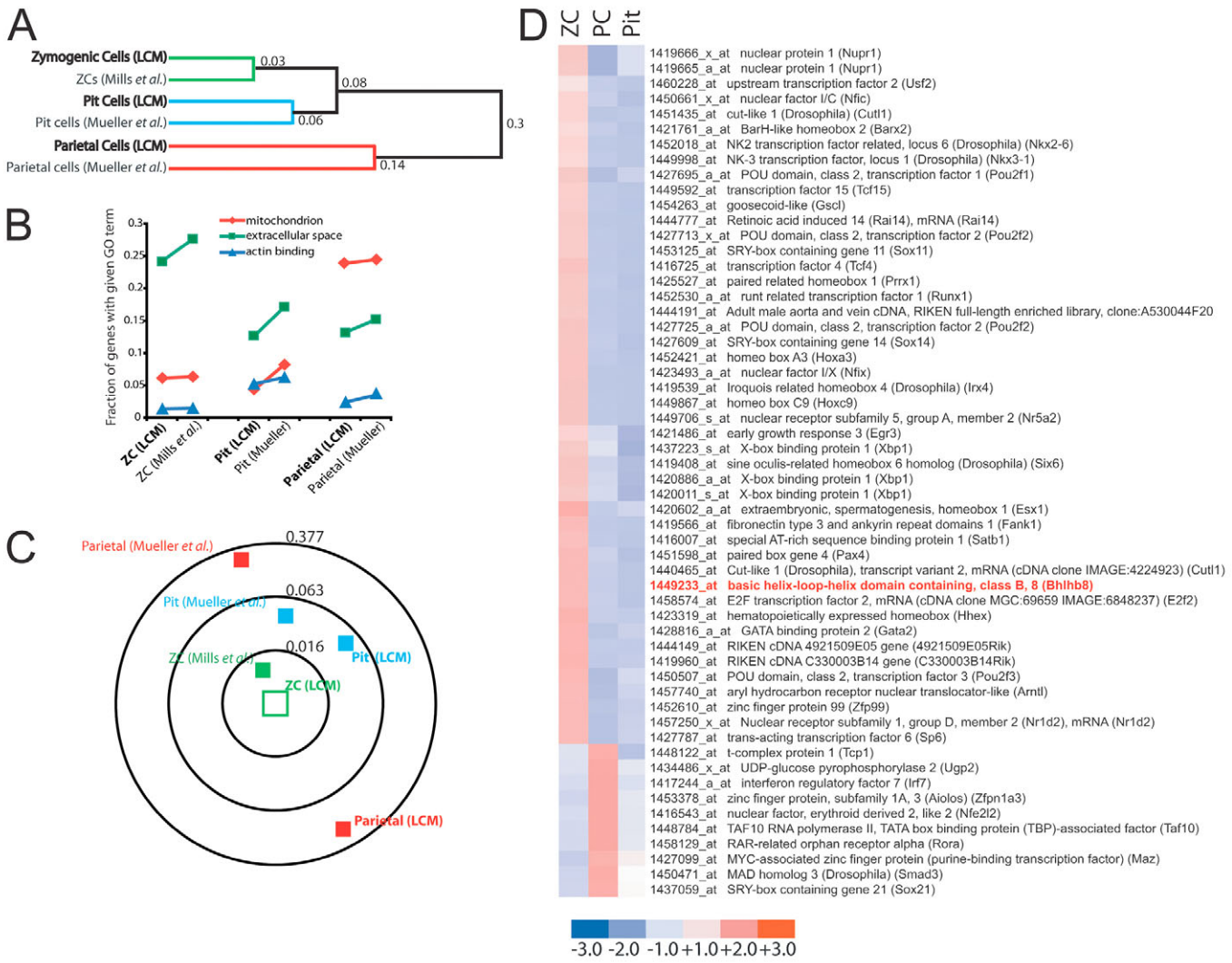

Fig. 2. GeneChips generated from laser-captured cells parallel earlier studies but additionally identify numerous transcription factor mRNAs specifically enriched in ZCs. (**A**) Dendrogram showing how gene expression profiles generated from laser-capture microdissected cells for the current study cluster with previous profiles of the same cell types. Numbers at branches are modified Pearson's correlations: where 0 means that profiles are identical, 1 means that they are wholly unrelated and 2 means that they are inversely related. Correlations were calculated by comparing the fractional representation of each GO term in each expression profile using GOurmet software (Doherty et al., 2006). LCM, laser-capture microdissected profiles in the current study; Mills et al., ZCs purified by digesting stomachs followed by centrifugation purification (Mills et al., 2003); Mueller et al., data from another previous study (Mueller et al., 2004). (**B**) Individual GO terms that differentiate each cell population have been selected to show how the types of genes enriched in each expression profile match known functions associated with those cell lineages. Genes described by the GO term 'extracellular space' are highly represented in profiles of ZCs with a function of secretion; those described by the term 'mitochondrion' are enriched in parietal cells, which are characterized by abundant mitochondria; those described as 'actin-binding' are most common in the rapidly migrating, cytoskeleton-fortified pit cells. (**C**) The same data as in A have been rendered to show the Pearson's correlation between the current ZC profile and all others. Note that the current ZC is most closely related to the previous ZC profile. (**D**) Heatmap of transcription-regulating genes with expression that is significantly enriched in either the LCM ZC or LCM parietal cell list.

the ZC marker channel (e.g. GIF) channel across the lassoed area. Values were blanked by subtracting MFIs in each channel for parietal cells (which do not label with either marker). Distribution of *Mist1* expression was quantified in wild-type mouse stomachs by staining with anti-Mist1, GSII and either anti-GIF or anti-Pgc. Every well-oriented gastric unit across the entire circumference of a random section through the mid-section of the corpus of each mouse was scored for GSII, GIF or Pgc, and Mist1. For the Brdu studies, four *Mist1*$^{-/-}$ and three age-matched *Mist1*$^{+/-}$ mice were injected intraperitoneally with a 15 μl/g live weight solution of 8 mg/ml bromodeoxyuridine and 0.8 mg/ml fluorodeoxyuridine (both from Sigma, St Louis, MO). Stains and counts were performed as for determination of Mist1 distribution.

Electron microscopy and secretory granule size determination

Freshly excised stomachs were flushed with Hepes-buffered RPMI medium, inflated with fixative (modified Karnovsky's, 2.5% glutaraldehyde, 2% paraformaldehyde in 0.1 mmol/l cacodylate buffer) in a fixative-filled flask. After overnight 4°C fixation, ~1 mm-thick, transverse stomach rings were cut from the mid-corpus region, and then ~1 × 1 mm-thick sections perpendicular to the ring axis were taken from the mid-corpus region; both greater and lesser curvature were sampled. Post-fixation was in 2% OsO_4 (in 0.1 mmol/l cacodylate buffer). Tissues were embedded in PolyBed 812 (Polysciences Inc., Warrington, PA); 90–100 nm sections were cut with a Diatome diamond knife and stained with uranyl acetate in 50% MeOH and Venable's lead citrate. Transmission EM was performed on a JEOL JEM

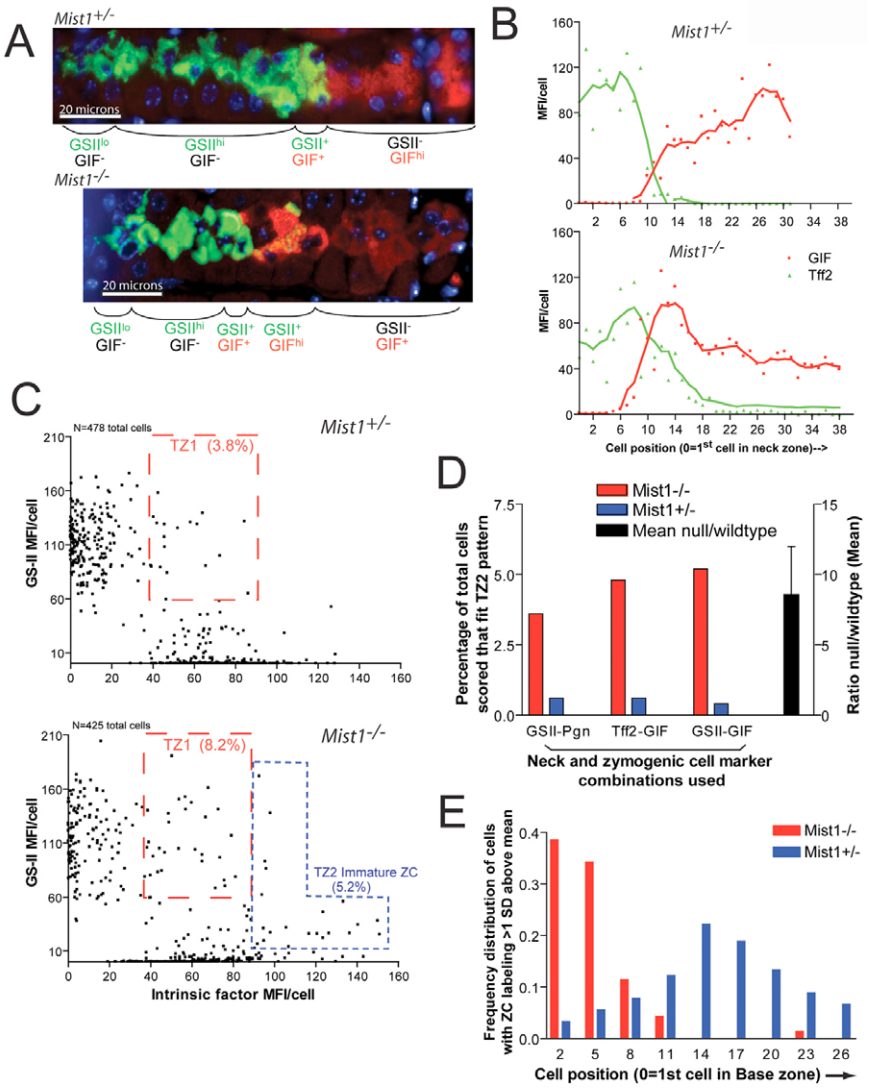

Fig. 3. *Mist1*$^{-/-}$ gastric units show increased numbers of neck-to-ZC transitional cells. (**A**) Neck and base zones of representative single gastric units are depicted (gastric lumen to left); mucous granules of neck cells are green (GSII lectin) and zymogenic granules of ZCs are red (GIF). Note GSII^{+}/GIF^{Hi} cells early in the base zone of the *Mist1*$^{-/-}$ mice. (**B**) MFI of all cells along the neck or ZC differentiation axis in single representative gastric units from each genotype, using anti-Tff2 as a neck cell marker and anti-GIF as a ZC marker, are graphed. The *x*-axis represents individual cells ordered as a function of distance from the stem cell; i.e. number 1 is the first Tff2^{+} cell in the upper neck zone, and the highest number designates the cell at the bottom of the base zone. Every cell is quantified with regard to both its mucus content (green) and zymogenic granule (red) content. Note the brief transition (cells 10-12) in the normal unit where cells have both mucous and zymogenic granules; otherwise wild-type cells have either exclusively mucous granules (i.e. are neck cells) or exclusively zymogenic granules (i.e. are ZCs in the base). The *Mist1*$^{-/-}$ unit (lower graph) has a longer transition zone (cells 9-16), and the cells at the basal side of the transition zone (cells 11-14) have abundant zymogenic granule staining but also retain mucous granules (these are immature ZCs or TZ2 cells corresponding to the GSII^{+}/GIF^{Hi} cells in A and C). Lines through datapoints generated by a curve-generating algorithm based on a running average of 'nine nearest neighbor' datapoints. (**C**) Scatter plots of all cells quantified in all mice, showing GSII (mucus) versus GIF (zymogen) levels. Red boxes show neck-to-ZC transitional cells of the first transition stage (TZ1), with GSII ⩾ mean neck cell GSII and GIF within 1 s.d. of mean ZC GIF. Fraction of total cells showing this phenotype is in parentheses. Blue box outlines the cluster of GIF^{Hi}GSII^{+} cells ('immature ZCs' or transition stage 2,'TZ2' cells) with GIF significantly above (i.e. ⩾1 s.d.) mean ZC GIF and GSII ⩾10 in *Mist1*$^{-/-}$ mice. Similar scatter plots were also generated for other marker combinations (Tff2-GIF and GSII-Pgc; not shown) (**D**) Fraction of cells with significantly above average (⩾1 s.d.) ZC marker staining and coexpression of above background (>10 MFI) neck cell marker expression (i.e. TZ2 cells). Black column shows mean ±s.d. of the ratio of the fractional representation of TZ2 cells between *Mist1*$^{-/-}$ and *Mist1*$^{+/-}$ animals. (**E**) Distribution as a function of cell position within the gastric unit of all cells with ZC marker expression ⩾1 s.d. above mean ZC MFI. Data are the sum across seven mice and 33 gastric units scored per genotype, using the three neck-ZC marker combinations. Cell 0 in this graph defined as the first cell in the gastric unit with ZC expression at or above the ZC mean and neck cell marker MFI <70 (i.e. the first cell at the neck-base interface). Note how *Mist1*$^{-/-}$ cells with high ZC marker expression are in early cells (i.e. those nearest the neck), whereas cells with high ZC marker expression tend to occur later in the *Mist1*$^{+/-}$ (as the ZCs mature and migrate into the base).

1200-EX microscope with AMT Advantage HR (Advanced Microscopy Techniques Corp., Danvers MA) high-speed, wide-angle 1.3 megapixel TEM digital camera. Granule area was calculated by measuring two perpendicular diameters for every vesicle from size-calibrated photomicrographs of well-oriented gastric units. At least 100 vesicles per cell differentiation state were scored.

RESULTS

Identification of Mist1 as a candidate regulator of ZC differentiation

To identify potential regulators of ZC differentiation, we isolated ZCs from their niche using LCM and profiled their global pattern of gene expression. To enhance dissection precision, we developed an RNA-preserving protocol that allowed direct, multiple, simultaneous immunolabeling of targeted cells in frozen sections using cell lineage markers (see Materials and methods).

To increase purity of the ZC isolation, we first individually captured and removed the potentially contaminating parietal cells that sporadically occur in the bases of gastric units before retrieving ZCs. For a reference control, we microdissected and pooled another population of parietal cells: those from the region above the neck zone of the gastric unit, where neither neck cells nor ZCs could contaminate the dissection. For a second reference population, we microdissected pit cells in the most apical portion of the pit zone, above the isthmus and neck of the gastric unit but below the gastric

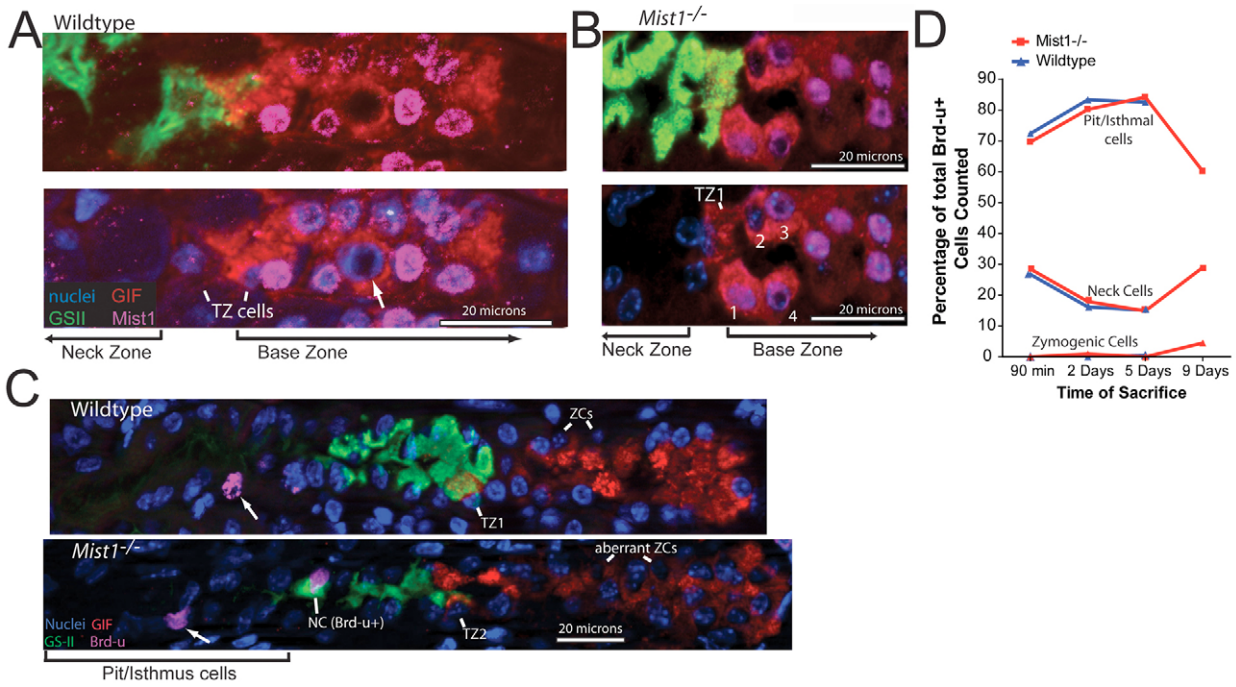

Fig. 4. Differentiation, proliferation and Mist1 expression in the gastric unit. (**A**) Expression of *Mist1* in the neck and base of wild-type animals was assessed: blue, nuclei (bisbenzimide); green, neck cells (GSII); red, ZCs (GIF); purple, poyclonal rabbit anti-Mist1. Upper: GSII, GIF and Mist1. Lower: same field with bisbenzimide, GIF and Mist1. Note how only cells that also express GIF (i.e. ZCs or transitional cells) express nuclear Mist1 and that almost all mature ZCs express Mist1. Two TZ cells are indicated with negative nuclei (although quantification showed that ~half of transitional cells are Mist1-positive). A single apparently negative ZC is marked by an arrow (these cells are rare). (**B**) Expression from the *Mist1* promoter in the *Mist1*$^{-/-}$ mice. Labeling and layout as in A, except: purple, expression of nuclear *lacZ* 'knocked in' to *Mist1* promoter (anti-β-galactosidase antibody). Note how *Mist1* promoter activity is first detectable in a subset (promoter-positive cells are labeled '1,3,4') of the four GIF^{Hi} cells at the transition between the neck and base zones and is not detectable in neck cells or the earlier transition cell with equal levels of mucous and zymogenic granules (TZ1). (**C**) Brdu immunolabeling in representative gastric units at 90 minute timepoint. Labeling as in A, except: purple, polyclonal goat anti-Brdu. Note single positive cell in isthmus or pit region of wild type and *Mist1*$^{-/-}$ (arrows) and early neck cell of *Mist1*$^{-/-}$ mouse. Transitional cells with negative nuclei are also indicated. (**D**) Brdu pulse-chase experiments. All animals were injected with Brdu concomitantly and sacrificed on different days. Note that the day 9 timepoint comprised only one genotype: *Mist1*$^{-/-}$.

surface to exclude all neck and parietal cells. RNA from each cell lineage (ZCs, pit cells and parietal cells, ~10 ng/cell lineage/mouse) was purified, linearly amplified and hybridized to Affymetrix MOE430v2 GeneChips.

To validate the gene expression profiles of our three cell populations, we wanted to quantitatively compare them to previously published expression profiles. However, previous profiles of these cell lineages contained varying numbers of genes and were generated using different methods (i.e. either on earlier versions of GeneChips or using entirely different microarray platforms). To circumvent these technical obstacles, we used a software suite we developed, called 'GOurmet' (Doherty et al., 2006), to annotate the genes preferentially expressed by a given cell type with the corresponding GO terms for each gene (Harris et al., 2004) and then compute the relative representation of each GO term in the list of genes as a whole. Because GO terms describe the functional properties of genes, this translation of expression profiles from a list of genes into a distribution of GO terms allowed us to quantitatively compare entire expression profiles at the level of the functions and properties of their component genes. Hence, comparisons were rendered essentially independent of methods used to generate the expression profile. Using this approach, we determined that our LCM-derived expression profiles paralleled the corresponding previously generated profiles (Fig. 2A,C), and the types of genes that were enriched in each cell lineage profile were consistent with the function of that cell (Fig. 2B).

Prior gene expression profiles of ZCs (Mills et al., 2003; Mueller et al., 2004), although informative about key functional aspects of these long-lived highly secretory cells (Fig. 2B), did not yield much insight about factors regulating ZC differentiation. By contrast, GOurmet analysis of the LCM-based expression profile of ZCs identified 41 genes that could be classified as having a known or putative role in transcription regulation (Fig. 2D). To narrow this list of possible ZC differentiation mediators for subsequent functional studies, we performed a bioinformatic metanalysis. We reasoned that, because ZCs are acinar secretory cells, transcription factors regulating their differentiation should also be enriched in serous salivary glands, in which the tissue parenchyma is almost exclusively composed of similar acinar cells. Thus, we screened a publicly available panel of adult mouse organ expression profiles (GEO Series GSE1986; http://www.ncbi.nlm.nih.gov/geo/query/acc.cgi?acc=GSE1986) for salivary gland-enriched mRNAs. Of our 41 ZC-enriched transcripts, only *Xbp1* and *Mist1* showed this pattern. As *Xbp1* is involved in the protein unfolding response and general ER maintenance in diverse tissues (Brewer and Hendershot, 2005), we

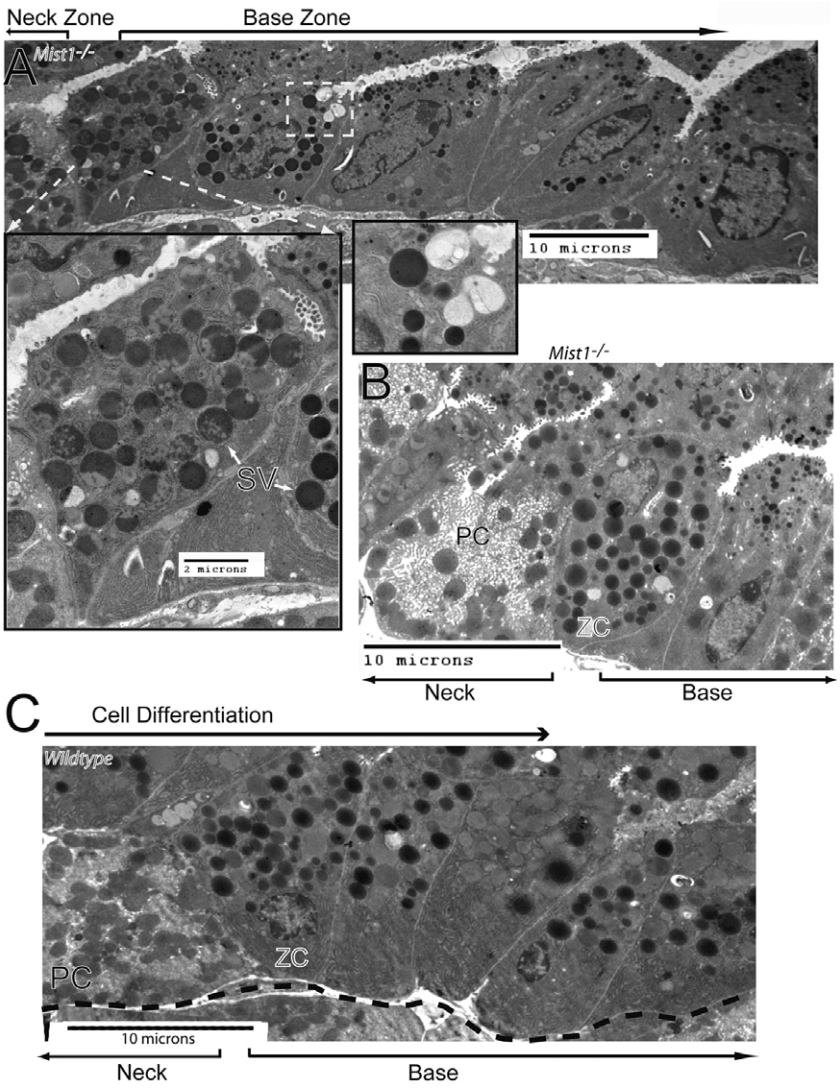

Fig. 5. ZCs in *Mist1*$^{-/-}$ mice abutting the neck zone (TZ2 cells) form normal serous granules but basal ZCs have fewer, smaller granules. (**A**) TEM of lower neck zone and upper base of a *Mist1*$^{-/-}$ gastric unit (neck zone to left). Notice how large, normal zymogenic granules occur only in cells immediately adjacent to the neck zone. A cell (TZ2, shown at higher magnification in the inset at left) with large, chimeric granules that are similar to those of normal ZCs but have a smaller electron-lucent mucus-like component as well (chimeric vesicle labeled SV, left arrow; normal vesicle indicated with arrow to right) occurs at the transition between the last parietal cell of the neck zone and the base. Outlined by a dashed box in A and shown at greater magnification in the right inset, adjacent to the TZ2 cell on the right is the highest ZC in the base; it has no residual mucus in its granules, but unlike a wild-type ZC, it has a mixture of large, normal zymogenic granules with occasional, abnormally small granules, and several granules appear in the process of fusing with the apical plasma membrane. In addition, in this region, there are invaginations of the apical plasma membrane, evidence of recently released granules. The remaining cells, farther away from the neck zone (i.e. to the right) are all abnormal: rather than having a pyramidal acinar cell morphology, they are cuboidal or columnar with irregular apical plasma membranes, and have scant supranuclear cytoplasm with abnormally small secretory granules. (**B**) Neck-to-base transition region in another *Mist1*$^{-/-}$ gastric unit from a section from another mouse. Again, note the abundant large granules in the immature ZC that is immediately adjacent to the last parietal cell of the neck zone and thus has not yet entirely entered the base. Residual mucus in the granules is not observed, but may be detectable by immunofluorescence; thus, this cell may either be a TZ2 cell or an early ZC. (**C**) Neck-to-base transition in a wild-type gastric unit for reference. Notice how all ZCs in this transition area (whether adjacent to neck zone or more mature) have large, abundant secretory granules. PC, last parietal cell of neck zone; ZC, immature ZC adjacent to neck zone.

excluded it from further analysis. Thus, we focused on *Mist1* as a potential key regulator of ZC differentiation and undertook a detailed analysis of its possible functional role in ZC development and maturation.

Molecular-morphological confirmation that ZCs arise from neck cells

Mice null for *Mist1* had been previously generated. Loss of Mist1 does not have long-term effects on viability or fertility in mice raised under standard conditions (Pin et al., 2001), and the effects of loss of Mist1 function are confined to the cells in which *Mist1* is normally expressed, making the *Mist1* mice an excellent tool for analysis of differentiation pathways in the adult gastric epithelium. To determine the cellular origins and development of ZCs in the presence or absence of *Mist1*, we first established a system for quantitative analysis of neck cell and ZC differentiation in the adult gastric unit. The lectin GSII (*Griffonia simplicifolia-II*) labels the mucous granules of neck cells intensely, and antibody against gastric intrinsic factor (GIF) labels the zymogenic granules of murine ZCs with corresponding intensity (Fig. 3A). In wild-type or *Mist1* heterozygous mice, the mucus-containing cells in the neck zone labeled exclusively with GSII, and the mature ZCs in the base zone labeled exclusively with GIF. We noted, however, a transition zone between the end of the neck zone and the beginning of the base that harbored a small number of cells with cytoplasm that contained both mucus and zymogens (Fig. 3A,B), consistent with the hypothesis that ZCs arise from neck cells that exchange mucous secretion for digestive enzyme secretion as they enter the base of the gastric unit. As ZCs migrated away from the neck, their GIF expression tended to increase, indicating a developmental gradient from the progenitor neck zone to the base of the gastric unit (Fig. 3A,B,C).

Loss of Mist1 leads to quantitative increase in neck-to-ZC transitional cells

Analysis of *Mist1* null mice showed that the transition cells at the end of the neck zone were markedly increased in abundance. Furthermore, the highest levels of GIF, the ZC marker, were seen within cells in the early base, immediately adjacent to the neck zone; GIF levels in cells that had migrated farther into the base were considerably lower (Fig. 3A,B,C). Thus, our data indicated that, although neck cell differentiation appeared normal, *Mist1*$^{-/-}$ mice had a defect in ZC maturation.

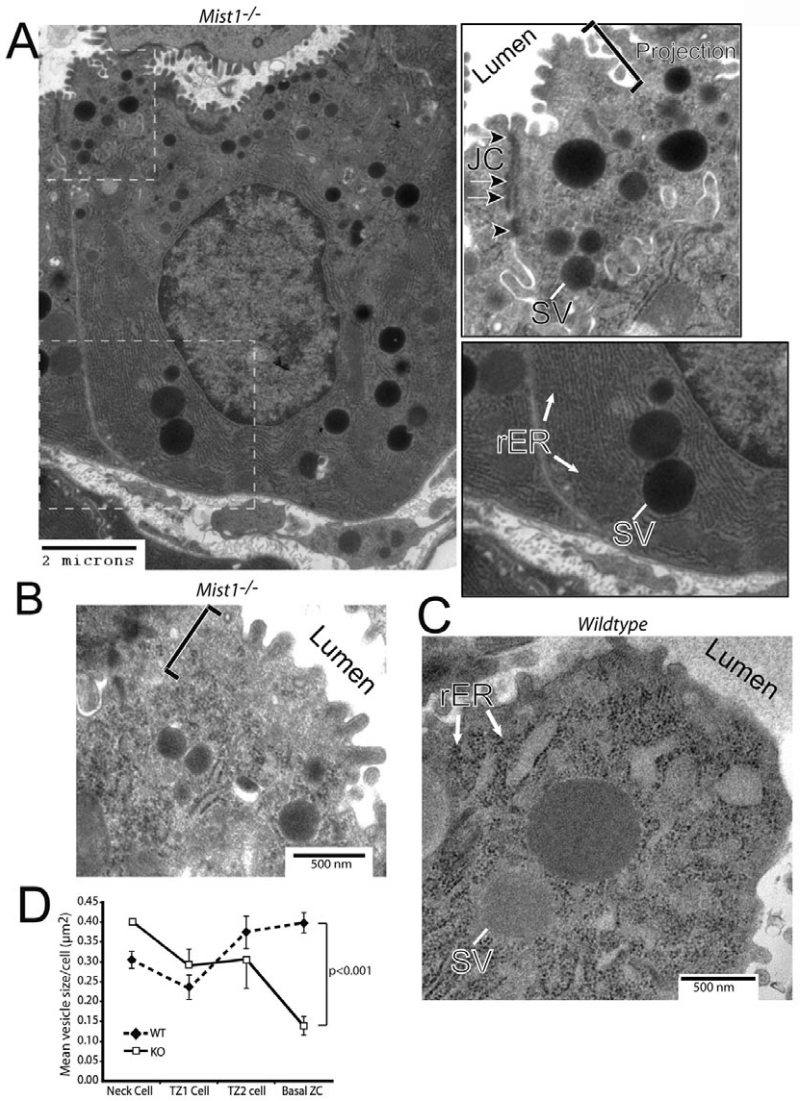

Fig. 6. ZCs in bases of *Mist1*$^{-/-}$ animals have substantial deficiencies in apical cytoplasmic development. (**A**) ZC from the base of a gastric unit in a *Mist1*$^{-/-}$ mouse. Upper right inset: normal apical tight (upper arrow, JC), adherens (lower arrows) and desmosomal (arrowhead) complexes and scattered, abnormally small secretory granules (SV). The apical plasma membrane is abnormally tufted with occasional surface blebs or projections (bracketed and labeled Projection). rER is disorganized apical to the nucleus, and there is a band ~500 nm thick of amorphous granular cytoplasm just beneath the apical plasma membrane. Bottom right inset: normal sized vesicles (SV) and abundant rER, indistinguishable from basolateral cytoplasm of wild-type ZCs. (**B**) Apical cytoplasm of another *Mist1*$^{-/-}$ ZC from the base of a different gastric unit showing scattered, scant rough ER and region of amorphous apical cytoplasm (bracketed). (**C**) Higher magnification of apical cytoplasm of the control mature ZC in Fig. 1D for reference, where large secretory vesicles and complex rER can be seen extending to the apical plasma membrane. (**D**) Mean area of secretory vesicles at each developmental stage is plotted. Statistically significant decrease in secretory vesicle size occurs in *Mist1*$^{-/-}$ mice relative to control only in basal ZCs (*P*-value by two-tailed Student's *t*-test).

To determine the extent of the increased abundance of transitional cells in *Mist1*$^{-/-}$ mice, we quantified ZC differentiation by measuring mean cytoplasmic fluorescent intensity in every cell expressing above background levels of neck cell markers and/or zymogenic cell markers in 33 gastric units in seven *Mist1*$^{-/-}$ and seven *Mist1*$^{+/-}$ mice. The data summed across ~1100 cells from each genotype using three combinations of neck and ZC markers (GSII and anti-GIF, GSII and anti-Pgc, anti-Tff2 and anti-GIF) quantified the substantially increased abundance of transitional cells coexpressing neck cell and ZC markers in *Mist1*$^{-/-}$ gastric units (Fig. 3C shows scatter plot for GSII-GIF; summed data for all markers in Fig. 3D). These transitional cells could be gated into two populations. The first was delineated by coexpression of approximately equal levels of neck cell and ZC markers (i.e. levels within 2 s.d. of mean ZC and mean neck cell marker levels). These cells (the GSII^{+}GIF^{+} pattern in Fig. 3A) showed a twofold increase in abundance (3.8 to 8.2% with GSII and GIF; 3.2 to 12.0% with Tff2 and GIF; 11.4 to 19.3% with GSII and Pgc; *P*-value by paired two-tailed *t*-test <0.033) in *Mist1*$^{-/-}$ mice (Fig. 3C, red dashed boxes). The second subset of transitional cells was characterized by high ZC marker expression (levels ⩾1 s.d. above the mean intensity for the ZC marker) with neck cell marker levels significantly above background (GSII^{+}GIF^{Hi} pattern in Fig. 3A, blue dashed box in Fig. 3C). These GSII^{+}GIF^{Hi}-type cells were nearly tenfold more abundant in *Mist1*$^{-/-}$ mice versus wild-type mice, no matter the combination of neck and ZC marker used (Fig. 3D, $P<0.017$).

Next, we determined the relative position of each transitional cell population within the gastric unit (Fig. 3A,B,E). This analysis indicated that the two transitional cell populations represented two sequential stages of transition between neck cells and ZCs. The GSII^{+}GIF^{+} (i.e. describing the cells with approximately equal levels of ZC and neck cell markers) population is the first transitional stage, as these cells were found predominantly at the end of the neck zone (e.g. Fig. 3A,B) in both *Mist1*$^{-/-}$ and control mice. We refer to these as transitional zone stage 1 (TZ1) cells. The GSII^{+}GIF^{Hi} pattern occurred at the interface between neck and base or early in the base in all three neck and ZC marker combinations (Fig. 3A,B,E); we designate this cell population (which was rare in wild-type mice) transitional zone stage 2 (TZ2) cells. Together, our data support the hypothesis that ZCs differentiate from neck cells and indicate that *Mist1* is required during neck to ZC differentiation, because, in its absence, there is accumulation of transitional cells with intermediate neck and ZC morphology.

If Mist1 is necessary for maturation of all ZCs from the neck cell zone, then all mature ZCs should express *Mist1* normally, and expression should be restricted to ZCs and perhaps transitional cells. To verify this, we quantified distribution of Mist1 in randomly selected gastric units from multiple mice using a polyclonal antibody against Mist1 (see, for example, Fig. 4A). Mist1 was seen in 97% of ZCs (1168 cells counted) and 47% of the cells coexpressing GSII and a ZC marker (123 cells counted). We have never observed Mist1 in neck cells; accordingly, 0 of 450 neck cells were Mist1-positive in this experiment. We also determined distribution of *Mist1* promoter activity in *Mist1*$^{-/-}$ mice, taking advantage of the nuclear-localized *lacZ* coding region that had been targeted to the *Mist1* null allele (Pin et al., 2001). In *Mist1* nulls, expression from the *Mist1* locus began in a subset of TZ2 cells (GSII^{+}/GIF^{Hi} TZ2 cells; Fig. 4B) abutting – but no longer within – the neck zone and was uniformly present in all ZCs that had migrated away from the neck and into the base. *Mist1* expression was rarely found in TZ1 cells (Fig. 4B).

The increase in cells with combined neck and ZC features at the border between the neck and base zones, in combination with the pattern of *Mist1* expression, suggested that Mist1 is required specifically for the terminal stage of ZC differentiation. A defect at that stage, when ZCs migrate fully into the base of the gastric unit, might result in a feedback increase in abundance of transitional forms at the interface between the neck and base. Also arguing for this interpretation is the observation that, as *Mist1*$^{-/-}$ ZCs migrate away from the neck zone and downregulate neck cell mucus, they concomitantly lose expression of differentiated ZC markers. Together, our analysis suggests that ZC differentiation normally occurs in four phases (see model in Fig. 7): (1) neck cell (GSII^{Hi}GIF^{-}); (2) early neck-to-ZC transitional zone cell ('TZ1' or GSII^{+}GIF^{+} cells); (3) early basal transitional zone cell ('TZ2' or GSII^{+}GIF^{Hi} cells); and (4) mature ZC (GSII^{-}GIF^{Hi}). Also, we conclude that Mist1 is required for cells to become normal terminal ZCs. In the absence of Mist1, TZ2 cells eventually exit the TZ2 stage, but never become mature ZCs, and instead accumulate various structural abnormalities.

There are alternative explanations of our results: (1) that the apparent transitional cells with coexpression of neck and ZC markers may represent a common progenitor cell from which both the neck and ZC arise; and/or (2) that these cells may be increased in *Mist1*$^{-/-}$ mice because loss of Mist1 leads to non-specifically increased proliferation rates that alter the differentiation pattern of the neck and ZC lineages. To address these possibilities, we performed pulse-chase labeling experiments with bromodeoxyuridine (Brdu), a thymidine analog that is permanently incorporated into replicating DNA strands of dividing cells. The results (Fig. 4C,D) indicate no difference in active sites of proliferation (as measured by distribution of Brdu-labeled cells at 90 minutes after injection) or migration of progenitor cells (i.e. distribution of Brdu label after chases of 2 and 5 days) between *Mist1*$^{-/-}$ and *Mist1*$^{+/-}$ mice (Pearson's correlation of the fractional distribution of Brdu label between the two genotypes was 0.999, where perfect correlation=1.0). Furthermore, total incorporation of label was almost identical at each timepoint between genotypes, (mean for *Mist1*$^{+/-}$ mice of 1.6±0.4 Brdu-positive cells/gastric unit and 1.3±0.4 for *Mist1*$^{-/-}$ mice), arguing strongly against a generalized increase in proliferation in *Mist1*$^{-/-}$ mice and confirming no experimental bias in Brdu levels injected or subsequent immunostaining. No label was identified within the neck-to-ZC transitional zone at any time during the experiment, and ZCs never constituted more than 1% of the labeled cells in either genotype at the first three timepoints. However, in a single *Mist1*$^{-/-}$ mouse followed for 9 days after Brdu injection, a small fraction (4.5%) of the aberrant, basal ZCs (see below) that formed in these mice began to show label incorporation, and, although they were not identified in the specific sections and counting parameters established for the multi-timepoint experiment in Fig. 4D, occasional labeled transitional cells could be found incidentally at this timepoint. Thus, the pattern of Brdu labeling in both genotypes of mice was consistent with published reports of normal gastric unit differentiation (Karam and Leblond, 1993a; Li et al., 1996), indicating that proliferative activity in the gastric unit occurs in the isthmus and pit zones, with a somewhat smaller fraction of neck cells also showing proliferative activity. Our results are also consistent with the hypothesis that ZCs arise only after a differentiation timecourse that takes many days following cessation of mitosis. Furthermore, the data indicate that the population of apparent neck-to-ZC transitional cells are not sites of active proliferation in *Mist1*$^{-/-}$ mice or controls and so they are unlikely to be a common progenitor for both the neck cells, which are themselves actively proliferating, and the ZCs, which do not appear to proliferate.

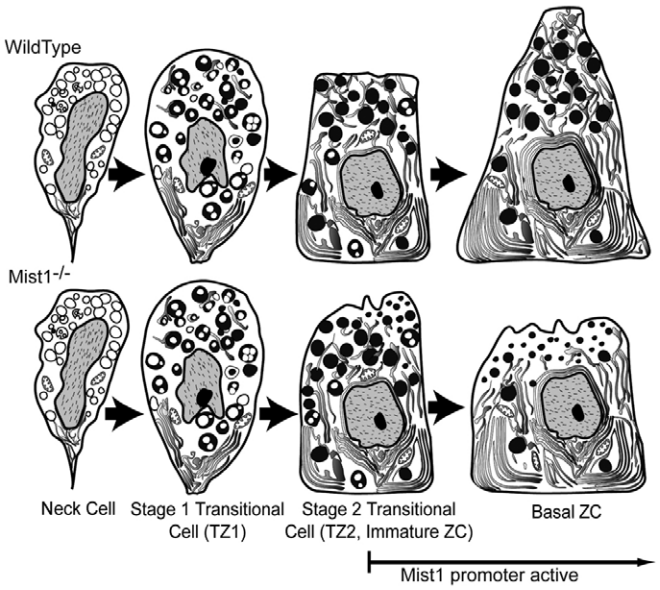

Fig. 7. Model of the ultrastructural mechanisms of ZC differentiation in wild-type and *Mist1*$^{-/-}$ mice. Mucous granules are white, serous granules are black and rER is shaded gray. The model shows that normal ZC differentiation involves transition of mucous into serous granules and that the final step involves extension and elaboration of apical cytoplasm. In *Mist1*$^{-/-}$ mice apical cytoplasms do not develop, and normal mature ZCs do not form.

TZ2 (immature zymogenic) cells in Mist1$^{-/-}$ stomachs have normal ultrastructure but do not become mature basal ZCs

Overall, the data argue that Mist1 does not have a role in initial specification of the ZC fate, because the *Mist1*$^{-/-}$ TZ2 cells express abundant markers of ZC differentiation (GIF, Pgc). In addition, cells of the ZC lineage can eventually migrate into the base and turn off expression of neck cell markers even in the absence of Mist1 (e.g. Fig. 3A,B; and note appearance of Brdu in ZC-marker-positive,

neck-cell marker negative cells at day 9 in Fig. 4D). However, ZC marker expression is clearly also lost as TZ2 cells migrate away from the neck (Fig. 3A,D,E), indicating that following the TZ2 stage, ZC differentiation is abnormal. Earlier published experiments in other tissues had suggested that Mist1 was necessary specifically for formation of the secretory apparatus in highly secretory exocrine cells (Pin et al., 2001; Johnson et al., 2004); however, the TZ2 cell phenotype, characterized by abundant expression of secretory zymogenic markers, also supports the argument against a role in secretory apparatus elaboration in ZCs. To help address these issues, we studied the pattern of ZC differentiation in *Mist1*$^{-/-}$ mice at the ultrastructural level using transmission electron microscopy (TEM). The development of zymogenic granules in representative differentiating wild-type ZCs is shown in Fig. 5C, and in Fig. S1 in the supplementary material. Note that the most immature ZC exiting the neck zone (Fig. 5C, the ZC adjacent to the parietal cell in the neck zone) contains abundant, large zymogenic granules, and subsequent more mature cells (to the right) maintain this level of granularity. Whereas immature ZCs also contained abundant, large granules in *Mist1*$^{-/-}$ mice, it is striking that, as ZCs migrated from the neck zone, they contained fewer and smaller granules (Fig. 5A,B; note that EM results are representative of nine blocks examined from three different *Mist1*$^{-/-}$ mice). The immature ZCs with abundant granules corresponded in morphology and location (i.e. nearest the neck zone) to the GSII^{+}GIF^{Hi} TZ2 population detailed in Fig. 3 (see left inset, Fig. 5A, where the cell contains abundant large secretory granules, some of which contain remnants of electron-lucent material, consistent with neck cell mucins). In addition, the TEM results showed that the pattern of decreased GIF staining as a function of ZC distance from the neck zone (Fig. 3A,B,E) accurately reflected the differentiation-related loss of secretory granules as a whole in *Mist1*$^{-/-}$ ZCs.

Thus, the results indicated uniform defects in *Mist1*$^{-/-}$ ZCs as they migrate away from the neck zone, and the ultrastructural defects correlate spatiotemporally with *Mist1* gene expression in wild-type mice (and expression of *lacZ* from the *Mist1* promoter in *Mist1*$^{-/-}$ ZCs; Fig. 4A,B). To assess in more detail how loss of Mist1 affected the final stage of ZC differentiation, we analyzed ZCs in the bases of *Mist1*$^{-/-}$ and wild-type mice in our TEM sections. We noted that normal ZCs elaborated their supranuclear cytoplasm in a coordinated extension of their apices with neighboring cells, such that ZCs at the base of a gastric unit were pyramidal or Erlenmeyer flask shaped with minimal luminal surface area (Fig. 1C,D).

However, examination of multiple *Mist1*$^{-/-}$ mice showed that the bases of their gastric units were devoid of mature ZCs. Basal *Mist1*$^{-/-}$ ZCs were cuboidal or cuboidocolumnar, with stunted supranuclear cytoplasm and extensive apical luminal surfaces (see cells at right in Fig. 5A or cell in Fig. 6A), indicating that neighboring ZCs had failed to coordinate extension of their apical cytoplasm. Without coordinated apical expansion, the lumens in the bases of gastric units as a whole were wider and resembled ducts more than the acinar, pouch-like structures of normal mice. *Mist1*$^{-/-}$ ZCs had significantly smaller (P<0.001, Fig. 6D), less abundant vesicles and their supranuclear rough endoplasmic reticulum (rER) network was sparse. Furthermore, they exhibited a reproducible, ~500 nm region of amorphous, organelle-free cytoplasm immediately subjacent to the plasma membrane (Fig. 6A,B), and their apical plasma membrane generally had a tufted, dynamic appearance that was in marked contrast with the smooth apical membranes of wild-type ZCs (Fig. 1D, Fig. 6C). Interestingly, the subnuclear and basolateral cytoplasm of *Mist1*$^{-/-}$ ZCs was indistinguishable from wild type, showing abundant lamellar rER and even occasional zymogenic granules of normal size (Fig. 6A). Junctional complexes also appeared normal (Fig. 6A).

Thus, our TEM observations confirmed our immunofluorescent data, indicating that immature TZ2 ZCs in *Mist1*$^{-/-}$ mice contained abundant, zymogenic granules of normal size and shape, further arguing against a role, at least in the stomach, of *Mist1* in generation of secretory granules or establishment of the core cellular secretion machinery (e.g. an elaborate rER network). Rather, the results support the argument that *Mist1* regulates genes needed for immature ZCs to undergo the apical morphological changes required for terminal differentiation into the mature, acinar cells at the base of the gastric unit.

DISCUSSION

Genetic evidence for ZC differentiation from neck cell precursors

The morphological aspects of ZC differentiation have been studied previously in normal mice. These studies indicated that ZCs arise from mucous neck cell precursors (Suzuki et al., 1983; Karam and Leblond, 1993c; Ge et al., 1998). However, before the current study, no gene required for any step in the differentiation of neck cells into mature, basal ZCs had been identified. Furthermore, it had been posited that the conversion of a mostly postmitotic, long-lived, terminally differentiated mucus-secreting cell into a serous secretory cell was highly unusual (Hanby et al., 1999). Our results show for the first time that deletion of a single gene, *Mist1*, blocks normal terminal ZC differentiation with all basal zymogen-secreting cells in *Mist1*$^{-/-}$ mice showing multiple structural defects. The block in terminal differentiation is accompanied by accumulation of cells at the interface between the neck and the base zones of the gastric unit. Those interface cells show coexpression of neck cell and ZC markers and clearly represent stages in the transition between the neck cell and ZC, thereby providing the first molecular-genetic evidence that ZCs arise from neck cells.

The mechanism of the Mist1$^{-/-}$ phenotype

Mist1$^{-/-}$ mice form cells with abundant zymogenic granules (TZ2 cells). They also still form aberrant ZCs in bases of *Mist1*$^{-/-}$ gastric units with basal cells expressing GIF and Pgc in the absence of neck cell markers. Thus, Mist1 is not necessary for initial conversion of mucus granules to zymogenic granules, and it is necessary neither for migration of nascent ZCs into the base nor for downregulation of neck cell markers. But in *Mist1*$^{-/-}$ mice there are no mature ZCs with abundant, large secretory granules, elaborate supranuclear cytoplasms and pyramidal, acinar cell shapes. Thus, *Mist1* is a developmentally regulated transcription factor that must be necessary for the terminal functional and structural maturation of ZCs (our interpretation of both normal ZC development and the aberrant development are modeled in Fig. 7).

The molecular mechanism of the defective differentiation phenotype in *Mist1*$^{-/-}$ mice will undoubtedly be complex: Mist1 is a transcription factor and may concomitantly activate multiple cellular pathways. A starting point for molecular analysis of the role of Mist1 might be to examine differences in cytoskeletal organization between *Mist1*$^{-/-}$ and wild-type ZCs. The tufted apical plasma membrane and organelle-free region of sub-apical cytoplasm in the defective *Mist1*$^{-/-}$ ZCs suggest that their apical cytoskeleton is hyperdynamic or hypercontractile. Abnormalities in the normal cytoskeletal lattice that regulates secretory granule release could explain both the loss of granules as *Mist1*$^{-/-}$ ZCs leave the neck zone and the failure in coordinated extension of the apical cytoplasm that these cells normally undertake as they mature.

Gastric epithelial niche-related regulation of Mist1 expression

Our results illustrate some of the advantages of the stomach as a model system for studying differentiation processes in a mammalian system with relevance to human disease. The quantitative ZC differentiation analysis system that we developed allowed us to detect a normally rare precursor population (i.e. the immature TZ2 ZC) and to tease out differences between those cells and the mature ZCs of the base. The analysis was greatly facilitated by the spatiotemporal organization of development in the stomach, where, unlike mouse pancreas (the other organ where *Mist1* has primarily been studied) or the *Drosophila* nervous system [in which the fly homolog *dimm* has been studied (Hewes et al., 2003)], cell-type differentiation can be followed in a stage-by-stage fashion in tissue sections even in adults.

Eventually, it will be important to establish whether Mist1 regulates identical genes in different organ systems (e.g. pancreas versus stomach). For example, it has been reported that *Mist1*$^{-/-}$ acinar cells of the pancreas undergo an age-related switch in differentiation state, in which serous, acinar cells begin to resemble pancreatic ductal cells in older mice (Zhu et al., 2004). Ductal cells have cuboidal morphology with scant supra-apical cytoplasm, similar to the morphology of the basal ZCs we observe in *Mist1*$^{-/-}$ mice, and because of the failure of ZCs to extend apical cytoplasms, the base zones of *Mist1*$^{-/-}$ mice resemble ducts more than acini. It will be interesting to determine whether basal ZCs in *Mist1*$^{-/-}$ mice aberrantly express duct markers and whether the abnormal duct-like cells in *Mist1*$^{-/-}$ pancreases show defects in cytostructural organization like those of ZCs in *Mist1*$^{-/-}$ stomachs.

In the stomach, the pattern of defective differentiation and the timing of *Mist1* expression both suggest that induction of *Mist1* occurs as transitional cells begin to exit from the neck. Migration from the neck involves migration away from direct cell-cell contact with parietal cells and from the factors they secrete, such as the morphogen Shh (Lees et al., 2005; Merchant, 2005). Parietal cells occupy most of the basement membrane surface in the neck zone (see, for example, Fig. 1C), so ZCs entering the base must rapidly expand their basal contact with the basement membrane. Either loss of parietal cell-mediated factors and/or increased exposure to factors in extracellular matrix (or possibly subjacent capillaries) could regulate induction of *Mist1* expression.

Relevance for human disease

An exigency for studying neck-to-ZC differentiation is that this developmental pathway is aberrant in the precancerous state of chronic gastric atrophy (Houghton et al., 2004; Katz et al., 2005; Nomura et al., 2005; Shiotani et al., 2005), and mucous neck-like cells form the bulk of tumor cells in diffuse-type, signet ring adenocarcinomas (Yamashina, 1986; Charlton et al., 2004). Despite the abundant evidence for aberrant ZC differentiation in carcinogenesis, little is known about the molecular and cellular details of the defects. Our current results should allow us to examine differentiation during carcinogenesis with greater molecular resolution. For example, *Mist1* expression could be used as a marker of definitive ZC differentiation and also might be lost as an early event in carcinogenesis.

Conclusion

Our data show how an approach that combines in situ cell purification with bioinformatics and detailed morphological analysis can take advantage of the spatiotemporal organization of the gastric unit to elucidate the molecular-genetic underpinnings of the development of a long-lived, slowly differentiating, secretory cell lineage. We argue that the organization of the stomach makes it a useful model system for studies of fundamental developmental processes in an adult mammal. Furthermore, because the stomach is an all too frequent site for pathophysiological differentiation processes (e.g. cancer), such studies may also often have the additional advantage of directly furthering our understanding of human disease.

For GeneChip hybridization, we thank the Multiplexed Gene Analysis Core of the Siteman Cancer Center (supported in part by NCI grant #P30 CA91842). We also thank the Washington University Digestive Diseases Research Core Center Murine Models Core, supported by grant #P30 DK52574. Further grant support: J.C.M. (K08 DK066062) and S.F.K. (R01 DK55489). Thanks also to Karen Green for EM assistance and to Drs Jim Skeath and Indira Mysorekar for thoughtful review of the manuscript.

Supplementary material

Supplementary material for this article is available at
http://dev.biologists.org/cgi/content/full/134/1/02700/DC1

References

Brewer, J. W. and Hendershot, L. M. (2005). Building an antibody factory: a job for the unfolded protein response. *Nat. Immunol.* **6**, 23-29.

Charlton, A., Blair, V., Shaw, D., Parry, S., Guilford, P. and Martin, I. G. (2004). Hereditary diffuse gastric cancer: predominance of multiple foci of signet ring cell carcinoma in distal stomach and transitional zone. *Gut* **53**, 814-820.

Doherty, J. M., Carmichael, L. K. and Mills, J. C. (2006). GOurmet: A tool for quantitative comparison and visualization of gene expression profiles based on gene ontology (GO) distributions. *BMC Bioinformatics* **7**, 151.

Falk, P., Roth, K. A. and Gordon, J. I. (1994). Lectins are sensitive tools for defining the differentiation programs of mouse gut epithelial cell lineages. *Am. J. Physiol.* **266**, G987-G1003.

Ge, Y. B., Ohmori, J., Tsuyama, S., Yang, D. H., Kato, K., Miyauchi, M. and Murata, F. (1998). Immunocytochemistry and in situ hybridization studies of pepsinogen C-producing cells in developing rat fundic glands. *Cell Tissue Res.* **293**, 121-131.

Hanby, A. M., Poulsom, R., Playford, R. J. and Wright, N. A. (1999). The mucous neck cell in the human gastric corpus: a distinctive, functional cell lineage. *J. Pathol.* **187**, 331-337.

Harris, M. A., Clark, J., Ireland, A., Lomax, J., Ashburner, M., Foulger, R., Eilbeck, K., Lewis, S., Marshall, B., Mungall, C. et al. (2004). The Gene Ontology (GO) database and informatics resource. *Nucleic Acids Res.* **32 Database issue**, D258-D261.

Hewes, R. S., Park, D., Gauthier, S. A., Schaefer, A. M. and Taghert, P. H. (2003). The bHLH protein Dimmed controls neuroendocrine cell differentiation in Drosophila. *Development* **130**, 1771-1781.

Houghton, J., Stoicov, C., Nomura, S., Rogers, A. B., Carlson, J., Li, H., Cai, X., Fox, J. G., Goldenring, J. R. and Wang, T. C. (2004). Gastric cancer originating from bone marrow-derived cells. *Science* **306**, 1568-1571.

Johnson, C. L., Kowalik, A. S., Rajakumar, N. and Pin, C. L. (2004). Mist1 is necessary for the establishment of granule organization in serous exocrine cells of the gastrointestinal tract. *Mech. Dev.* **121**, 261-272.

Karam, S. M. (1993). Dynamics of epithelial cells in the corpus of the mouse stomach. IV. Bidirectional migration of parietal cells ending in their gradual degeneration and loss. *Anat. Rec.* **236**, 314-332.

Karam, S. M. and Leblond, C. P. (1993a). Dynamics of epithelial cells in the corpus of the mouse stomach. I. Identification of proliferative cell types and pinpointing of the stem cell. *Anat. Rec.* **236**, 259-279.

Karam, S. M. and Leblond, C. P. (1993b). Dynamics of epithelial cells in the corpus of the mouse stomach. II. Outward migration of pit cells. *Anat. Rec.* **236**, 280-296.

Karam, S. M. and Leblond, C. P. (1993c). Dynamics of epithelial cells in the corpus of the mouse stomach. III. Inward migration of neck cells followed by progressive transformation into zymogenic cells. *Anat. Rec.* **236**, 297-313.

Karam, S. M. and Leblond, C. P. (1993d). Dynamics of epithelial cells in the corpus of the mouse stomach. V. Behavior of entero-endocrine and caveolated cells: general conclusions on cell kinetics in the oxyntic epithelium. *Anat. Rec.* **236**, 333-340.

Karam, S. M., Yao, X. and Forte, J. G. (1997). Functional heterogeneity of parietal cells along the pit-gland axis. *Am. J. Physiol.* **272**, G161-G171.

Karam, S. M., Straiton, T., Hassan, W. M. and Leblond, C. P. (2003). Defining epithelial cell progenitors in the human oxyntic mucosa. *Stem Cells* **21**, 322-336.

Katz, J. P., Perreault, N., Goldstein, B. G., Actman, L., McNally, S. R., Silberg, D. G., Furth, E. E. and Kaestner, K. H. (2005). Loss of Klf4 in mice causes altered proliferation and differentiation and precancerous changes in the adult stomach. *Gastroenterology* **128**, 935-945.

Lees, C., Howie, S., Sartor, R. B. and Satsangi, J. (2005). The hedgehog signalling

pathway in the gastrointestinal tract: implications for development, homeostasis, and disease. *Gastroenterology* **129**, 1696-1710.
Li, C. and Wong, W. H. (2001). Model-based analysis of oligonucleotide arrays: expression index computation and outlier detection. *Proc. Natl. Acad. Sci. USA* **98**, 31-36.
Li, Q., Karam, S. M. and Gordon, J. I. (1996). Diphtheria toxin-mediated ablation of parietal cells in the stomach of transgenic mice. *J. Biol. Chem.* **271**, 3671-3676.
Luo, X., Shin, D. M., Wang, X., Konieczny, S. F. and Muallem, S. (2005). Aberrant localization of intracellular organelles, Ca^{2+} signaling, and exocytosis in Mist1 null mice. *J. Biol. Chem.* **280**, 12668-12675.
Merchant, J. L. (2005). Inflammation, atrophy, gastric cancer: connecting the molecular dots. *Gastroenterology* **129**, 1079-1082.
Mills, J. C., Andersson, N., Stappenbeck, T. S., Chen, C. C. and Gordon, J. I. (2003). Molecular characterization of mouse gastric zymogenic cells. *J. Biol. Chem.* **278**, 46138-46145.
Mueller, A., Merrell, D. S., Grimm, J. and Falkow, S. (2004). Profiling of microdissected gastric epithelial cells reveals a cell type-specific response to *Helicobacter pylori* infection. *Gastroenterology* **127**, 1446-1462.
Nomura, S., Yamaguchi, H., Ogawa, M., Wang, T. C., Lee, J. R. and Goldenring, J. R. (2005). Alterations in gastric mucosal lineages induced by acute oxyntic atrophy in wild-type and gastrin-deficient mice. *Am. J. Physiol. Gastrointest. Liver Physiol.* **288**, G362-G375.
Pin, C. L., Bonvissuto, A. C. and Konieczny, S. F. (2000). Mist1 expression is a common link among serous exocrine cells exhibiting regulated exocytosis. *Anat. Rec.* **259**, 157-167.
Pin, C. L., Rukstalis, J. M., Johnson, C. and Konieczny, S. F. (2001). The bHLH transcription factor Mist1 is required to maintain exocrine pancreas cell organization and acinar cell identity. *J. Cell Biol.* **155**, 519-530.
Rukstalis, J. M., Kowalik, A., Zhu, L., Lidington, D., Pin, C. L. and Konieczny, S. F. (2003). Exocrine specific expression of Connexin32 is dependent on the basic helix-loop-helix transcription factor Mist1. *J. Cell Sci.* **116**, 3315-3325.
Shiotani, A., Iishi, H., Uedo, N., Ishiguro, S., Tatsuta, M., Nakae, Y., Kumamoto, M. and Merchant, J. L. (2005). Evidence that loss of sonic hedgehog is an indicator of *Helicobater pylori*-induced atrophic gastritis progressing to gastric cancer. *Am. J. Gastroenterol.* **100**, 581-587.
Suzuki, S., Tsuyama, S. and Murata, F. (1983). Cells intermediate between mucous neck cells and chief cells in rat stomach. *Cell Tissue Res.* **233**, 475-484.
Yamashina, M. (1986). A variant of early gastric carcinoma. Histologic and histochemical studies of early signet ring cell carcinomas discovered beneath preserved surface epithelium. *Cancer* **58**, 1333-1339.
Zhong, S., Li, C. and Wong, W. H. (2003). ChipInfo: Software for extracting gene annotation and gene ontology information for microarray analysis. *Nucleic Acids Res.* **31**, 3483-3486.
Zhu, L., Tran, T., Rukstalis, J. M., Sun, P., Damsz, B. and Konieczny, S. F. (2004). Inhibition of Mist1 homodimer formation induces pancreatic acinar-to-ductal metaplasia. *Mol. Cell. Biol.* **24**, 2673-2681.